



## $^{29}\text{Si}$ high resolution solid state nuclear magnetic resonance spectroscopy of porous silicon

T. Pietraß<sup>a,\*</sup>, A. Bifone<sup>a</sup>, R.D. Roth<sup>b</sup>, V.-P. Koch<sup>b</sup>, A.P. Alivisatos<sup>a</sup>, A. Pines<sup>a</sup>

<sup>a</sup> *Materials Sciences Division, Lawrence Berkeley Laboratory and Department of Chemistry, University of California at Berkeley, Berkeley, CA 94720, USA*

<sup>b</sup> *Physik Department E 16, Technische Universität München, D-85747 Garching, Germany*

Received 22 August 1995; revised 4 December 1995

### Abstract

Porous silicon has been characterized by  $^{29}\text{Si}$  nuclear magnetic resonance spectroscopy under conditions of static samples, magic angle spinning, decoupling and cross polarization. In a free induction decay experiment, two  $^{29}\text{Si}$  resonances at  $-80$  and  $-111$  ppm were obtained. Cross polarization resulted in a single resonance at  $-97$  ppm. Magic angle spinning and decoupling slightly reduce the linewidth of the  $^{29}\text{Si}$  cross polarized signal. The minor narrowing effect and the relaxation behavior in the laboratory and rotating frame indicate a homogeneous contribution to the linewidth. The relaxation data suggest that the resonance observed under cross polarization conditions arises from  $\text{SiH}$  or  $\text{SiH}_2$  structural elements.

### 1. Introduction

In the controversy [1] about the origin of the luminescence of porous silicon, different mechanisms or combinations of mechanisms have been discussed: the presence of siloxene [2–4], quantum confinement [5,6], and surface states [7,8]. Thus, a study of the surface structure of porous silicon is important to substantiate current models. NMR spectroscopy provides information about local bonding configurations and, thus, constitutes a useful tool for the study of surface structures. Proton, deuterium and  $^{29}\text{Si}$  CP MAS (cross polarization [9] under magic angle spinning) nuclear magnetic resonance (NMR)

spectroscopy have been applied to amorphous silicon prepared under varying synthetic conditions.  $^1\text{H}$  and  $^2\text{H}$  NMR make it possible to distinguish between covalently bound protons in a dilute or clustered phase and molecular hydrogen [10–12];  $^1\text{H}$  multiple quantum NMR has been used to determine proton cluster sizes [13].  $^2\text{H}$  NMR studies on deuterated amorphous silicon a-Si:D,H confirm the existence of weakly bound deuterium in plasma deposited materials [14].  $^{29}\text{Si}$  CP MAS gives rise to distinguishable chemical shifts for amorphous and amorphous-microcrystalline mixed-phase hydrogenated silicon [15] and for varying hydrogen contents in amorphous silicon [16].

Porous silicon is synthesized by anodic etching of silicon wafers in hydrofluoric acid solution, which results in a coverage of the surface with hydrogen [17]. We are particularly interested in the surface of

\* Corresponding author. Present address: Department of Chemistry, New Mexico Tech, Socorro, NM 87801, USA. Tel.: +1-505 835 5586; fax: +1-505 835 5364; e-mail: tanja@nmt.edu.

the material. An indirect NMR surface study, using optically enhanced xenon as a surface probe, yielded information about adsorption properties and pore size distribution of the material [18]. In this work, we present data obtained by using  $^1\text{H}$  to  $^{29}\text{Si}$  cross polarization [9] in combination with magic angle spinning, which allows us to detect selectively the  $^{29}\text{Si}$  NMR resonances of the silicon atoms which are in close proximity to protons, namely, the silicon atoms residing on the surface of the material. Determination of the spin lattice and spin–spin relaxation times in the rotating frame provides information about the character of the line broadening and the magnitude of the dipolar interactions.

## 2. Experimental

The free-standing porous silicon was prepared by anodic etching of B-doped silicon wafers with a current density of  $30 \text{ mA/cm}^2$  in 48% hydrofluoric acid solution. The wafers were etched with the (100) surface exposed. Resistivities of the wafers were in the range of  $4.5$  to  $6 \ \Omega \text{ cm}^{-1}$ , corresponding to a carrier concentration of  $2$  to  $3 \times 10^{15} \text{ cm}^{-3}$  [19]. Transmission electron microscope images revealed characteristic nanocrystalline dimensions of about  $200 \text{ nm}$  for the described experimental conditions.

The material was powdered for NMR characterization. Two samples, prepared in different batches,

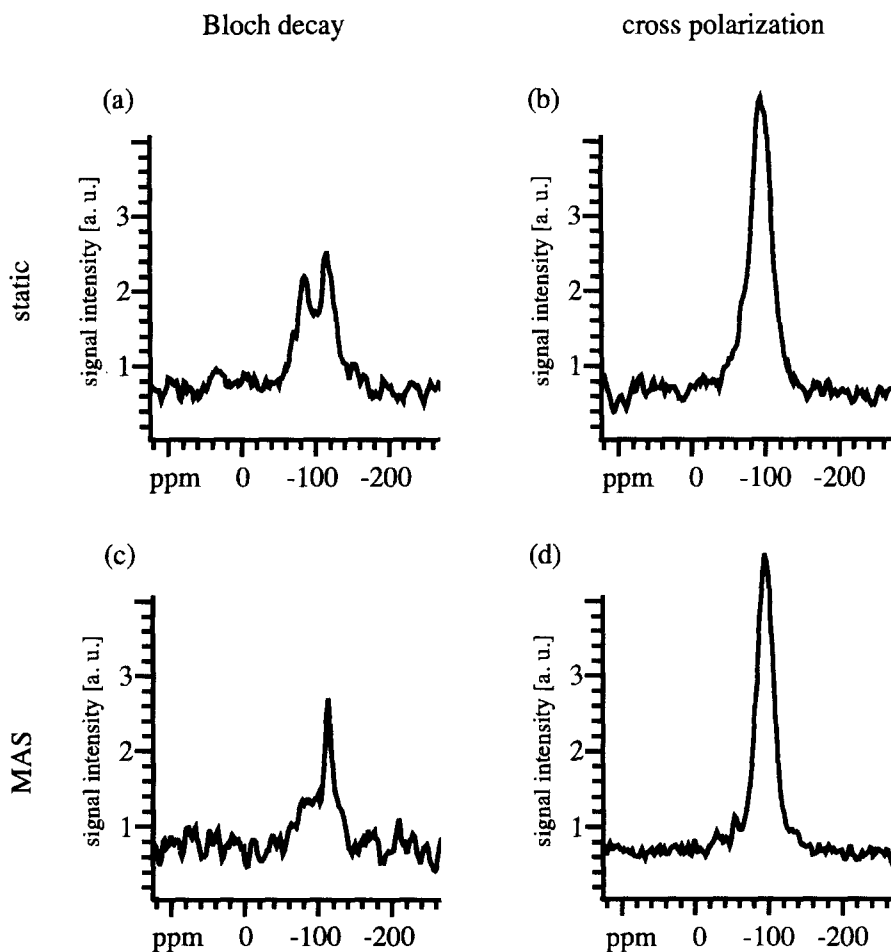


Fig. 1.  $^{29}\text{Si}$  NMR spectra of porous silicon under different acquisition conditions. The chemical shift of the cross polarization resonance does not correspond to any of the resonances in the static Bloch decay spectrum. The spinning speed in the MAS spectra is  $2.65 \text{ kHz}$ .

were kept in an inert atmosphere before being used in the NMR experiments and yielded consistent NMR results. After the NMR experiments, one of the samples was exposed to air for 2 months. IR spectra revealed a surface oxidation of about 10%. This sample is referred to as 'aged'.

NMR spectra were recorded with a home-built NMR spectrometer equipped with a 8.52 T superconducting magnet, corresponding to Larmor frequencies of 71.938 MHz and 362.133 MHz for  $^{29}\text{Si}$  and  $^1\text{H}$ , respectively. The radiofrequency field amplitudes of both the  $^1\text{H}$  and the  $^{29}\text{Si}$  channels were 25 kHz. In cross polarization experiments, 1000 to 4000 transients were accumulated with a recycle delay of 2 s and a duration of the contact pulse of 1 to 2 ms. The samples were spun in 7 mm aluminum oxide rotors of the Doty design. Compressed air was used as a driving and bearing gas. All spectra were recorded at ambient temperature.  $^{29}\text{Si}$  NMR chemical shifts are referenced to an external standard of tetramethylsilane. Chemical shifts were determined from Lorentzian fits to the NMR lineshape with a precision of  $\pm 1$  ppm.

### 3. Results

In Fig. 1, the  $^{29}\text{Si}$  NMR spectra of porous silicon obtained from a single pulse excitation (a, c) are compared with those from  $^1\text{H}$  to  $^{29}\text{Si}$  cross polarization (b, d). Spectra (a, b) were recorded under static conditions and without proton spin decoupling. Whereas the single pulse excitation (a) results in two predominant resonances, only a single line is present in the CP spectrum (b). For the resonances in spectrum (a), chemical shift values of  $-80$  and  $-111$  ppm were found, for the CP resonance (b)  $-97$  ppm. The effect of magic angle spinning at 2.65 kHz is also shown in Fig. 1 in spectrum (c) for single pulse excitation and (d) for cross polarization. Apart from a slight narrowing of the CP resonance, the effect of spinning is much stronger on the single pulse spectrum. The resonance at  $-80$  ppm has lost intensity with respect to the resonance at  $-111$  ppm.

The effect of line narrowing through proton decoupling and magic angle spinning is summarized for various experimental conditions in Table 1. Decoupling and spinning did not result in any observ-

Table 1  
Linewidths for  $^{29}\text{Si}$  NMR signals of porous silicon under different acquisition conditions

Acquisition conditions	$^1\text{H}$ decoupling	Linewidth (kHz) $\pm 0.02$ kHz
Static	no	2.42
	yes	2.10
1.87 kHz MAS	no	1.85
	yes	1.54
2.65 kHz MAS	no	1.60
	yes	1.55

able narrowing effect on the spectra obtained by single pulse excitation.

The dependence of the signal intensity upon the contact time in the CP experiments is plotted in Fig. 3 for the freshly prepared and aged samples. The aged sample presents the longest relaxation rate,  $T_{\text{Si-H}}$ . Fig. 4 summarizes the data for  $^1\text{H}$  and  $^{29}\text{Si}$  spin-lattice relaxation times in the rotating frame ( $T_{1\rho}$ ) and spin-spin relaxation times in the laboratory frame ( $T_2$ ), which were obtained with the basic pulse sequences by Alla and Lippmaa [20]. The dependence of the signal intensity on the dephasing time in a dipolar dephasing experiment [21] is shown in Fig. 5. For short dephasing times, an increased signal intensity can be observed when the rotor period is a multiple of the dephasing time.

### 4. Discussion

#### 4.1. Chemical shifts

One of the two dominant resonances of the free induction decay spectrum (a) in Fig. 1 could be assigned to silicon in the bulk, and the other one to silicon on the surface of the material. Then only the 'surface peak' should be enhanced by cross polarization. However, the shift of the CP peak is different from the shifts of the two dominant lines obtained by a single pulse Bloch decay.

Likely structural elements which give rise to the observed chemical shifts are Si-Si, Si-H, Si-OH and Si-O due to possible surface oxidation of the material. Bulk silicon resonates at  $-85$  ppm (static) [22] or  $-81$  ppm (MAS) [23]. For amorphous sili-

con, assignments to regions with dilute hydrogen of around  $-40$  ppm were proposed and to regions with clustered hydrogen of around  $-80$  ppm [15]. Another study reports  $^{29}\text{Si}$  chemical shifts for amorphous silicon with varying hydrogen contents in the range of  $-60$  to  $-90$  ppm [16]. For a completely hydrogen saturated silicon atom ( $\text{SiH}_4$ ), the shift moves upfield from the bulk silicon to  $-92.5$  ppm [24]. On the surface of silica gel, the geminal silanol peak was assigned a chemical shift of  $-89$  ppm and the single silanol of  $-99$  ppm. Silicon in siloxane, which results from the condensation of two adjacent silanol groups [25], resonates at  $-109$  ppm. Correspondingly, the interior hydroxyl groups in silica gel gave rise to a  $^{29}\text{Si}$  NMR shift of  $-99$  ppm for a  $Q_3$  silicon,  $-89$  ppm for a  $Q_2$  and  $-109$  ppm for a  $Q_4$  silicon atom [26,27].

For p-type bulk silicon with a carrier concentration in the range of  $10^{14}$  to  $10^{16}$   $\text{cm}^{-3}$ , spin–lattice relaxation times of 200 to  $> 300$  min are reported [28]. The single pulse Bloch decay spectrum (a) in Fig. 1 was acquired with an interval of 10 s between  $90^\circ$  pulses, and it is, therefore, highly unlikely that the resonance at  $-80$  ppm originates from the bulk of the porous silicon. We assume that both resonances are caused by silicon atoms which are close to the surface, at which a more efficient relaxation mechanism than in the bulk dominates. Dipolar relaxation caused by the interaction with dangling bonds or protons is a plausible mechanism. Although relaxation due to dangling bonds should be highly efficient [29], its contribution will only be minor, since the number of dangling bonds is on the order of  $10^{16}$   $\text{cm}^{-3}$  [8].

The bulk of our mesoscopic material with respect to the bulk material of a macroscopic three-dimensional silicon crystal differs considerably in spatial extensions. However, in mono-crystalline regions of our mesoscopic material, the  $^{29}\text{Si}$  NMR spin lattice relaxation time should not differ substantially from that of a three-dimensional crystal, since dipolar interactions decrease with the cubed distance of the nuclei to the relaxing centers. The longest range dipolar interaction possible for a  $^{29}\text{Si}$  nucleus in the material under study is with unpaired electrons. Even though the magnetic moment of an electron is larger than that of a nucleus by a factor of approximately  $10^3$ , for a nucleus–electron distance of only five

atomic layers ( $\sim 10$  Å), the resulting interaction would be reduced to the one of a nearby  $^{29}\text{Si}$  nucleus. Therefore, we conclude that only nuclei in close proximity to the surface are subject to an increased relaxation rate.

Spectrum (c) in Fig. 1 reveals a loss in intensity upon magic angle spinning for the resonance at  $-80$  ppm with respect to the resonance at  $-111$  ppm. This loss can have two possible origins: (i) an increase in the spin lattice relaxation time or (ii) the presence of a chemical shift anisotropy. In the latter case, the peak at  $-80$  ppm is attributed to one of the singularities of a uniaxial chemical shift powder pattern. In the former case, the spin lattice relaxation time must be dominated by dipolar interactions which are reduced upon spinning. This reduction is only expected for strong dipolar interactions such as between  $^{29}\text{Si}$  and  $^1\text{H}$ . In this case, the resonance must be observable under CP conditions. Therefore, we attribute the peak at  $-80$  ppm to a singularity of a chemical shift tensor. An Si–O structural element is most likely to cause a chemical shift anisotropy of the Si. Assuming that the powder pattern is uniaxial and covers the full width of the spectrum, the chemical shift anisotropy is estimated  $\Delta\sigma = 46$  ppm with an isotropic shift of  $-96$  ppm. Large chemical shift anisotropies of  $^{29}\text{Si}$  have been observed for  $Q_3$  silicon atoms, e.g., in a potassium tetrasilicate glass of more than 200 ppm [30].

#### 4.2. Proton decoupling

Decoupling and spinning did not result in any observable narrowing effect on the spectra obtained by single pulse excitation (Table 1). Hence, there is no strong proton coupling connected to the two dominant resonances, which is in agreement with the fact that they are not observable under CP conditions. Under cross polarization conditions, a small decrease in the linewidth with increasing spinning speed,  $\nu_{\text{rot}}$ , and upon proton decoupling can be observed. At  $\nu_{\text{rot}} = 2.65$  kHz, proton decoupling has no observable narrowing effect. Although the spinning speed exceeds the linewidth under static conditions, the narrowing effect is only minor, and no spinning sidebands can be observed. Therefore, the linewidth cannot be purely inhomogeneously broadened as is typical of the chemical shift anisotropy and dipolar

interactions between unlike spins [31]. High power proton decoupling under CP conditions results in a much stronger signal intensity than in the proton coupled spectra. Coupled and decoupled  $^{29}\text{Si}$  NMR CP MAS spectra for two different spinning speeds are shown in Fig. 2. A broad resonance which is effectively narrowed by decoupling contributes to the dominant CP resonance at  $-97$  ppm.

#### 4.3. Cross polarization dynamics and relaxation

The cross polarization relaxation times,  $T_{\text{Si-H}}$ , were shorter ( $0.10 \pm 0.1$  ms at  $\nu_{\text{rot}} = 1.95$  kHz and  $0.51 \pm 0.04$  ms at  $\nu_{\text{rot}} = 1.77$  kHz) for the freshly prepared samples than for the aged samples (Fig. 3)

and indicate a strong coupling between the protons and the silicons. At spinning speeds comparable to the static linewidth, a more efficient polarization transfer is expected for slower spinning speeds, since the dipolar interactions are averaged less efficiently. However, in the presence of homonuclear dipolar couplings, proton spin diffusion renders the polarization transfer less efficient with faster spinning speed [25] which is in agreement with the observed result. Moreover, the degree of surface oxidation is probably more advanced in the sample with  $T_{\text{Si-H}} = 0.51$  ms, a result consistent with the longer  $T_{\text{Si-H}}$  of the aged sample of  $0.93 \pm 0.10$  ms. For silicas, in which the protons are not directly bound to the silicon atoms, but are present as hydroxyl groups, a  $T_{\text{Si-H}}$

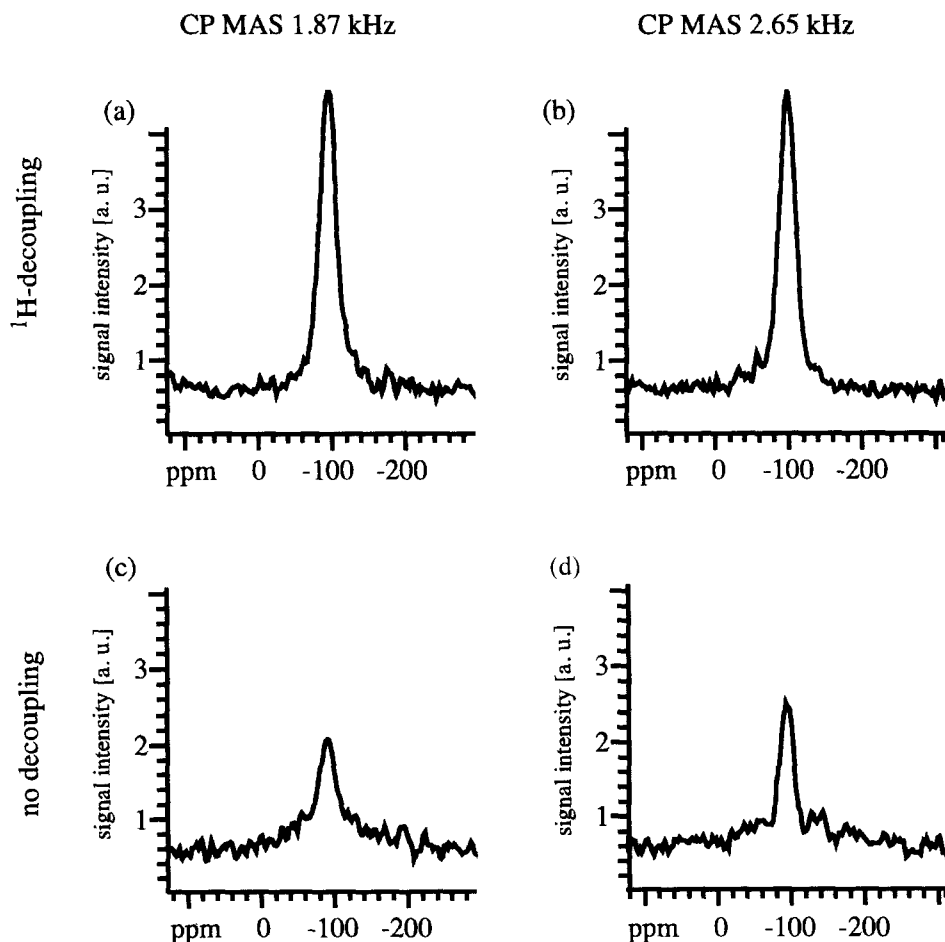


Fig. 2.  $^{29}\text{Si}$  NMR spectra of porous silicon with and without proton decoupling for different spinning speeds under otherwise identical experimental conditions.

of 2.3 ms, 2.9 ms and 12.9 ms for  $Q_2$ ,  $Q_3$  and  $Q_4$  silicon atoms was measured [26]. In siloxanes, the cross polarization relaxation time is much longer due to the increased distance to the protons [26,27]. It can, therefore, be concluded that the short relaxation times determined in the freshly prepared samples must originate from silicon atoms which are bound directly to protons.

Spin relaxation times are summarized in Fig. 4. The protons are characterized by a  $T_{1\rho}({}^1\text{H})$  of  $15.5 \pm 0.8$  ms ( $\nu_{\text{rot}} = 1.95$  kHz) and  $8.9 \pm 0.4$  ms ( $\nu_{\text{rot}} = 2.65$  kHz), when a monoexponential decay of the polarization is assumed. These values are of a similar magnitude to those observed for the protons of the interior protons of a silica gel [27]. The proton  $T_{1\rho}$  values are much longer than the  $T_{\text{Si-H}}$  values, so that they are of minor importance for efficient polarization transfer. A better fit resulted when the  $T_{1\rho}({}^1\text{H})$  data were analyzed in terms of a biexponential decay. For both spinning speeds, a faster relaxing

sample regime characterized by a  $T_{1\rho}({}^1\text{H})$  of 6 ms was found, and a slower one with a  $T_{1\rho}({}^1\text{H})$  of  $12.8 \pm 1.1$  ms at  $\nu_{\text{rot}} = 2.65$  kHz and of  $47.8 \pm 3.8$  ms at  $\nu_{\text{rot}} = 1.95$  kHz. Deviations from a monoexponential decay are typical of many-proton systems [29], in agreement with a surface coverage of the sample with protons.  $T_{1\rho}({}^{29}\text{Si})$  is only  $60.1 \pm 1.9$  ms, an indication that relaxation of the silicon spins is highly efficient in the presence of the local proton dipolar fields. The rapid loss of phase coherence of the protons, with a time constant,  $T_2({}^1\text{H})$ , of  $30.6 \pm 2.9$  ms, is an indication of strong homonuclear couplings among the protons. The spin-spin relaxation time,  $T_2({}^{29}\text{Si})$ , was determined in two different ways. In the first method, the sequence described in Ref. [32] was applied. After the contact pulse, the silicons process for a variable time in the dipolar fields of the protons and are then detected under proton decoupling. The dipolar fields on the silicons are created either by directly bound protons or through spin

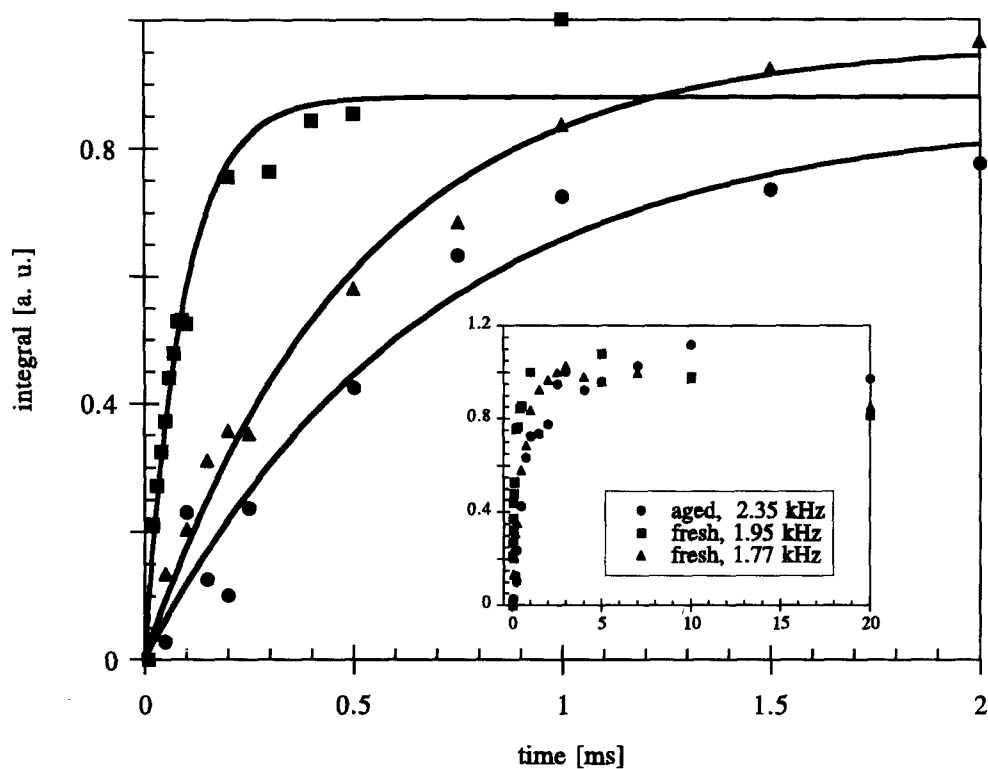


Fig. 3. Cross polarization relaxation rates  $T_{\text{Si-H}}$  for two freshly prepared and an aged porous silicon sample shown in detail for the first 2 ms. The curves correspond to the results of fits to an equation  $f(t) = c \cdot (1 - \exp(-t/T_{\text{Si-H}}))$ , with time,  $t$ , and a constant,  $c$ . The complete data set is shown in the inset. Numbers in kHz refer to the rotational frequency.

diffusion by neighboring protons [32]. The strength of the dipolar interaction is not solely determined by the inverse of the cubed distance between the two coupled nuclei, but can be mitigated by effects like molecular motion and  $^1\text{H}$ – $^1\text{H}$  or  $^{29}\text{Si}$ – $^{29}\text{Si}$  spin diffusion [25,32]. At 2.65 kHz,  $T_2(^{29}\text{Si})$  is  $57.9 \pm 1.7$  ms. In  $^{13}\text{C}$  dipolar dephasing experiments, methylene resonances can be suppressed by applying a dephasing time of typically 35 ms, for aliphatic methine carbons of about 55 ms. For methyl and unprotonated carbons, dephasing times on the order of 100 ms are required [21]. Dipolar interactions for the corresponding silicon structural elements are expected to be smaller, since the gyromagnetic ratio of  $^{29}\text{Si}$  is smaller than that of  $^{13}\text{C}$  and silicon has a larger covalent radius than carbon, which increases the internuclear distance to bound protons. Correspondingly, the dipolar dephasing times for  $^{29}\text{Si}/^1\text{H}$

are expected to be longer than for  $^{13}\text{C}/^1\text{H}$  in analogous structural elements. Therefore, it can be excluded that the time constant,  $T_2(^{29}\text{Si})$ , found for porous silicon originates from a structural element in which the proton is not directly bound to the silicon atom. A high mobility, as in a methyl group, is not expected, since the silicon atoms are embedded in the surface structure in the lattice, which is at least two-dimensional [18].

In the second method, a  $\pi$  pulse is inserted in the dephasing period on both channels [33], resulting in the refocusing of chemical shifts and other static field inhomogeneities [21]. In combination with magic angle spinning, the isotropic part of the chemical shift refocuses for any dephasing time,  $\tau$ , whereas the anisotropic part refocuses completely only when  $2\tau$  is an *even* multiple of the rotational frequency [25]. If the dipolar interaction changes

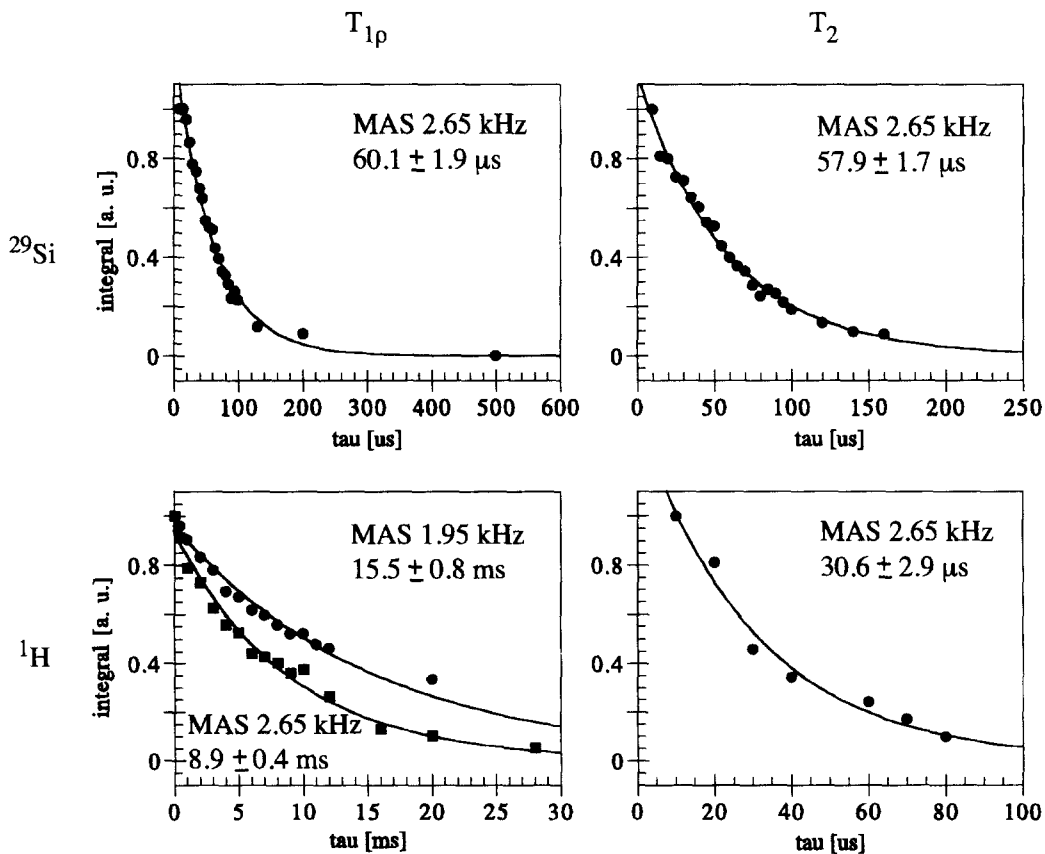


Fig. 4. Relaxation data of  $^{29}\text{Si}$  and  $^1\text{H}$  in the rotating and laboratory frame. The curves show the result of exponential fits to the equations  $f(\tau) = c \cdot \exp(-\tau/T_{1\rho})$  for  $T_{1\rho}$  and  $f(\tau) = c \cdot \exp(-\tau/T_2)$  for  $T_2$ , respectively.

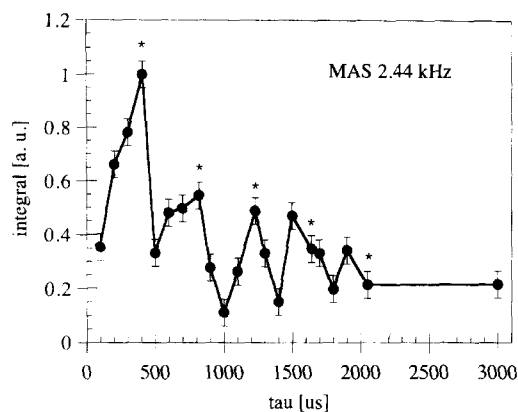


Fig. 5. Dipolar dephasing experiment with refocusing pulse. The line serves as a guide to the eye. Integer multiples of the rotational frequency (2.44 kHz) are marked with an asterisk.

within one rotor period due to chemical exchange, molecular motion or spin diffusion, it can no longer be refocused, not even at even multiples of a rotor period. The inhomogeneous part of the dipolar interaction refocuses completely when  $2\tau$  is a multiple of  $\nu_{\text{rot}}$  [25]. The weak narrowing effect on the linewidth introduced by magic angle spinning under CP conditions shows that chemical shift anisotropy is not a dominant interaction for porous silicon. The result of this experiment performed on the porous silicon is presented in Fig. 5. Multiples of the rotor period are marked with an asterisk. For short dephasing periods, an oscillatory behavior is evident with maxima at multiples of the rotation frequency. At dephasing times,  $2\tau > 3\nu_{\text{rot}}$ , the oscillations are less pronounced. Within the experimental error, the maxima cannot be clearly identified anymore with multiples of the rotation frequency.

## 5. Conclusions

Although the Fourier transformed signals provide only little information about the origin of the peaks, a detailed analysis of the relaxation behavior in the rotating and laboratory frame yields a consistent picture which allows the assignments of the resonances. The two resonances observed in a single pulse free induction decay experiment cannot originate from the crystalline bulk of the material but must be due to silicon atoms which have a much

shorter relaxation time. The two resonances are attributed to silicons in the proximity of dangling bonds, protons, or oxygen atoms. It should be noted that interactions with dangling bonds are long range and might also affect silicon atoms which are several layers away from the surface in the bulk. The proximity to protons can be excluded, since the two resonances cannot be observed under cross polarization conditions. The chemical shifts of the observed resonances suggest the assignment of the resonance at  $-80$  ppm to Si close to dangling bonds or oxygen, and the one at  $-111$  ppm to a  $Q_4$  silicon atom, since it is not visible under cross polarization conditions. The signal observed under cross polarization at  $-97$  ppm is assigned to a SiH or SiH<sub>2</sub> structural element, which is consistent with an upfield shift from the bulk silicon as observed previously in SiH<sub>4</sub>.

A quantification of the different species contributing to the signals was impossible due to the different relaxation times. Attempts to determine the long relaxation times failed because of signal to noise limitations. Future work will involve investigations of samples with different degrees of surface oxidation.

## Acknowledgements

This work was funded by the Director, Office of Energy Research, Office of Basic Energy Sciences, Materials Sciences Division, US Department of Energy, under Contract Number DE-AC03-76SF00098. A.B. thanks the ENI s.p.a., the foundation A. della Riccia and LBL for financial support.

## References

- [1] D.J. Lockwood, *Solid State Commun.* 92 (1994) 101.
- [2] M.S. Brandt, H.D. Fuchs, M. Stutzmann, J. Weber and M. Cardona, *Solid State Commun.* 81 (1992) 307.
- [3] S. Banerjee, K.L. Narasimhan, P. Ayyub, A.K. Srivastava and A. Sardesai, *Solid State Commun.* 84 (1992) 691.
- [4] S.L. Friedmann, M.A. Marcus, D.L. Adler, Y.-H. Xie, T.D. Harris and P.H. Citrin, *Appl. Phys. Lett.* 62 (1993) 1934.
- [5] Y.H. Xie, W.L. Wilson, F.M. Ross, J.A. Mucha, E.A. Fitzgerald, J.M. Macaulay and T.D. Harris, *J. Appl. Phys.* 71 (1991) 2403.



- [6] G. Mauckner, W. Rebitzer, K. Thonke and R. Sauer, *Solid State Commun.* 91 (1994) 717.
- [7] M.B. Robinson, A.C. Dillon, D.R. Haynes and S.M. George, *Appl. Phys. Lett.* 61 (1992) 1414.
- [8] F. Koch, V. Petrova-Koch and T. Muschik, *J. Lumin.* 57 (1993) 271.
- [9] A. Pines, M.G. Gibby and J.S. Waugh, *J. Chem. Phys.* 59 (1973) 569.
- [10] J.B. Boyce and S.E. Ready, *Physica B* 170 (1991) 305.
- [11] D.J. Leopold, J.B. Boyce, P.A. Fedders and R.E. Norberg, *Phys. Rev. B* 26 (1982) 6053.
- [12] J.B. Boyce, N.M. Johnson, S.E. Ready and J. Walker, *Phys. Rev. B* 46 (1992) 4308.
- [13] J. Baum, K.K. Gleason, A. Pines, A.N. Garroway and J.A. Reimer, *Phys. Rev. Lett.* 56 (1986) 1377.
- [14] V.P. Bork, P.A. Fedders, D.J. Leopold, R.E. Norberg, J.B. Boyce and J.C. Knights, *Phys. Rev. B* 36 (1987) 9351.
- [15] S. Hayashi, K. Hayamizu, S. Yamasaki, A. Matsuda and K. Tanaka, *J. Appl. Phys.* 60 (1986) 1839.
- [16] M.K. Cheung and M.A. Petrich, *J. Appl. Phys.* 73 (1993) 3237.
- [17] P.C. Searson, J.M. Macaulay and S.M. Prokes, *J. Electrochem. Soc.* 139 (1992) 3373.
- [18] T. Pietraß, A. Bifone and A. Pines, *Surf. Sci.* 334 (1995) L730.
- [19] S.M. Sze, *Physics of Semiconductor Devices* (Wiley, New York, 1981).
- [20] M. Alla and E. Lippmaa, *Chem. Phys. Lett.* 37 (1976) 260.
- [21] L.B. Alemany, D.M. Grant, T.D. Alger and R.J. Pugmire, *J. Am. Chem. Soc.* 105 (1983) 6697.
- [22] G.R. Holzmann, P.C. Lauterbur, J.H. Anderson and W. Koth, *J. Chem. Phys.* 25 (1956) 172.
- [23] J.S. Hartman, M.F. Richardson, B.L. Sherriff and B.G. Winstorow, *J. Am. Chem. Soc.* 109 (1987) 6059.
- [24] J.R.V. Wazer, C.S. Ewig and R. Ditchfield, *J. Phys. Chem.* 93 (1989) 2222.
- [25] I.-S. Chuang, D.R. Kinney, C.E. Bronnimann, R.C. Zeigler and G.E. Maciel, *J. Phys. Chem.* 96 (1992) 4027.
- [26] G.E. Maciel and D.W. Sindorf, *J. Am. Chem. Soc.* 102 (1980) 7606.
- [27] I.-S. Chuang, D.R. Kinney and G.E. Maciel, *J. Am. Chem. Soc.* 115 (1993) 8695.
- [28] R.G. Shulman and B.J. Wyluda, *Phys. Rev.* 103 (1956) 1127.
- [29] H. Pfeifer, *NMR Basic Principles and Prog.*, Vol. 7, ed. P. Diehl, E. Fluck and K. Kosfeld (Springer, Berlin, 1974) p. 53.
- [30] I. Farnan and J.F. Stebbins, *J. Am. Chem. Soc.* 112 (1990) 32.
- [31] M.M. Maricq and J.S. Waugh, *J. Chem. Phys.* 70 (1979) 3300.
- [32] S.J. Opella and M.H. Frey, *J. Am. Chem. Soc.* 101 (1979) 5854.
- [33] G. Bodenhausen, R.E. Stark, D.J. Ruben and R.G. Griffin, *Chem. Phys. Lett.* 67 (1979) 424.